Contrib. Astron. Obs. Skalnaté Pleso **47**, 151 – 156, (2017)

Detection of X-ray spectra and images by Timepix

M. Urban, O. Nentvich, V. Stehlikova and L. Sieger

Czech Technical University in Prague, Faculty of Electrical Engineering
Technicka 2, Prague 166 27, Czech Republic
(E-mail: urbanm24@fel.cvut.cz)

Received: May 11, 2017; Accepted: June 28, 2017

Abstract. X-ray monitoring for astrophysical applications mainly consists of two parts - optics and detector. The article describes an approach based on a combination of Lobster Eye (LE) optics with Timepix detector. Timepix is a semiconductor detector with 256×256 pixels on one electrode and a second electrode is common. Usage of the back-side-pulse from an common electrode of pixelated detector brings the possibility of an additional spectroscopic or trigger signal. In this article are described effects of the thermal stabilisation, and the cooling effect of the detector working as single pixel.

Key words: X-ray – Spectrum – Timepix detector – Lobster Eye optics

1. Introduction

Many tasks of recent astrophysics require to observe celestial X-ray sources over the wide field of view and wide spectral range. The possibility to detect the spectrum of source together with its image is a logical requirement of planned astronomical X-ray experiments.

Due to the significant attenuation of X-ray radiation when passing through the atmosphere, most measurements are placed above it. Numerous satellites have already been launched for this reason, and more missions are planned.

As examples of successfull missions can be mentioned Chandra (Weisskopf et al., 2000; Schwartz, 2014) and XMM Newton (Jansen et al., 2001) satellite or eRosita (Merloni et al., 2012) as mission in preparation. All these missions use the Wolter-I type of X-ray optics (Wolter, 1952) and Charge-coupled device (CCD) X-ray detector. Thermal noise minimization is required for a CCD detector to maximise spectral resolution. It is achieved by cooling to temperatures approximately from -60 to -100 degrees Celsius. This requirement causes the disadvantage in high energy consumption or the need of a cooling medium.

Another way to observe celestial X-ray sources with imaging device is a combination of Lobster Eye optics with Timepix detector. It can bring a wider field of view and lower requirements for thermal stabilisation of the detector, but only moderate angular resolution.

2. Experiments

There are many different ways to use Lobster Eye (LE), in astronomy (Hudec et al., 2015; Pína et al., 2016) and also in other fields of research, like colliders and medicine.

Czech CubeSat VZLUSAT-1 can be mentioned as an example. This small satellite has an X-ray optics and several payloads for testing carbon fibre reinforced plastic onboard. It is prepared to launch in June 2017 (Urban et al., 2016; Pina et al., 2015). This satellite carries the wide-field monitor demonstrator based on Lobster Eye optics with Timepix detector (Daniel et al., 2016; Dániel et al., 2016; Baca et al., 2016; Blazek et al., 2017).

Other example is in the proposed rocket experiment based on LE optics and the Timepix detector for wide-field sensing (Dániel et al., 2017).

3. X-ray detector - Timepix

The Timepix detector is a pixel-particle-counting detector. It is a hybrid pixel detector with (256 x 256) pixels with a pitch of 55 μm, therefore the detection area has 196 square millimetres. This detector consists of a silicon semiconductor bump-bonded to Complementary Metal-Oxide-Semiconductor (CMOS) readout circuit. Each pixel has its own charge sensitive preamplifier, threshold discriminator and 14 bit counter. Timepix detector have approx. 3 keV threshold without any upgrades. (Esposito et al., 2011; Llopart et al., 2007)

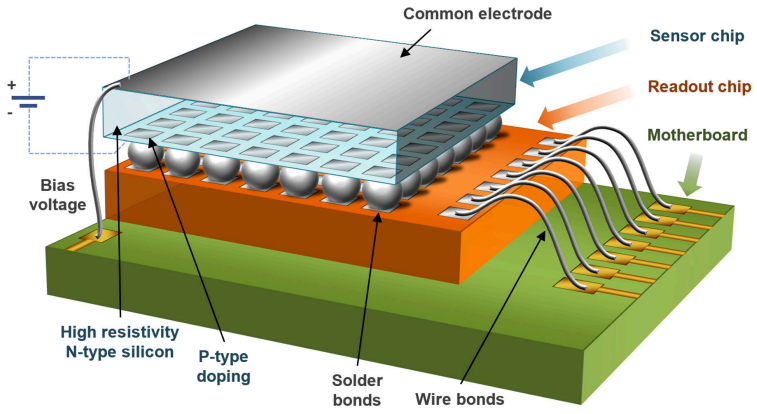

Figure 1. The hybrid semiconductor device Timepix (Platkevic, 2014; Urban et al., 2017)

One of the improvements can be a usage of a back-side-pulse and thermal stabilisation. (Platkevic et al., 2011; Holik et al., 2016) The silicon chip is equipped with a single backside electrode (common electrode in Fig. 1) from the opposite side than the matrix, where the bias voltage is connected as well. The signal from this common electrode can be used for the X-ray detection as well. If we use a detector from this side, it behaves like a one-pixel detector instead of the matrix of (256 x 256) pixels on the other side. The advantage of this approach is that we can use the signal from a larger detection area without the noise generated by the readout electronics under the chip. The disadvantage is that the capacity of the reading cell is noticeably higher, making it significantly more demanding for the reading electronics, mainly for the first stage of the preamplifier.

The Timepix detector is an uncooled and temperature unstabilised detector in standard usage. The signal is affected by two kinds of noises, thermal and electronic readout noise. Thermal noise is generated in the small pixels and can be reduced by acquisition time and cut by the threshold, which is set individually for each pixel. The major noise in the Timepix is generated by readout of pixels. This kind of noise is generated directly by bump-bonded application-specific integrated circuit (ASIC) chip on the silicon detection layer and readout interface (Platkevic et al., 2011).

In case the ASIC electronics of the detector is turned off, and the common back-side electrode is used, the reading noise is minimised. Measurement by the common electrode is then affected by the thermal noise error caused only. This measurement can cause inaccuracies because the noise characteristics of the detector vary with its temperature. One of the possibilities for an improvement of the Full Width at Half Maximum (FWHM) of the signal, the noise reducing and thus shifting the threshold to lower energy values is thermal stabilisation or cooling. Low-energy photons incident can be detected by Timepix3 as well. This generation of the Timepix detector has the minimum threshold around ~ 400 - $500\,e^-$, which corresponds with ~ 1.5-2 keV with a silicon sensor. (Turecek et al., 2016; Frojdh et al., 2015; Poikela et al., 2014)

3.1. Thermal stabilisation

The charge sensitive amplifier is one of the most important parts for signal evaluation and spectral resolution. The accuracy depends on the amplifier's FWHM respectively on detector capacitance and its thermal noise. The measurement setup in Fig. 2 was used for measurement. With respect to the limits of measuring facility, the energy corresponding to 109.7 keV was selected for principle verification. It is connected across the detector to the amplifier. Pulses are generated with frequency of 50 Hz. The amplified signal is shaped and connected to the Multichannel Analyzer (MCA) where is sorted into one of the 8 192 channels.

The measurements were performed at the room temperature 25 °C and at the temperature below the freezing point. The detector with the amplifier was

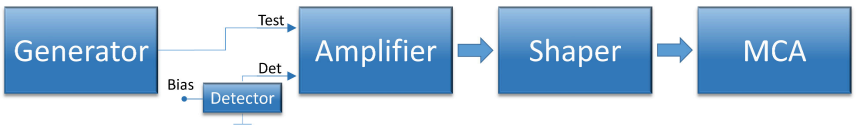

Figure 2. Principle of measurement

placed in a controlled environment at temperature -12 °C and protected against the water condensation during cooling.

The detector's FWHM can be determined from the equation (1)

$$N = \sqrt{N_{Det}^2 + N_{Amp}^2} \tag{1}$$

where N is total FWHM of the system, N_{Det} is the FWHM of the detector and N_{Amp} is the FWHM of the system with an amplifier without the detector.

From the equation (1) we express N_{Det}, which is our demanded value of FWHM. Values N and N_{Amp} are substituted by the measured values for each temperature as well. The results of measurement are listed in Tab. 1.

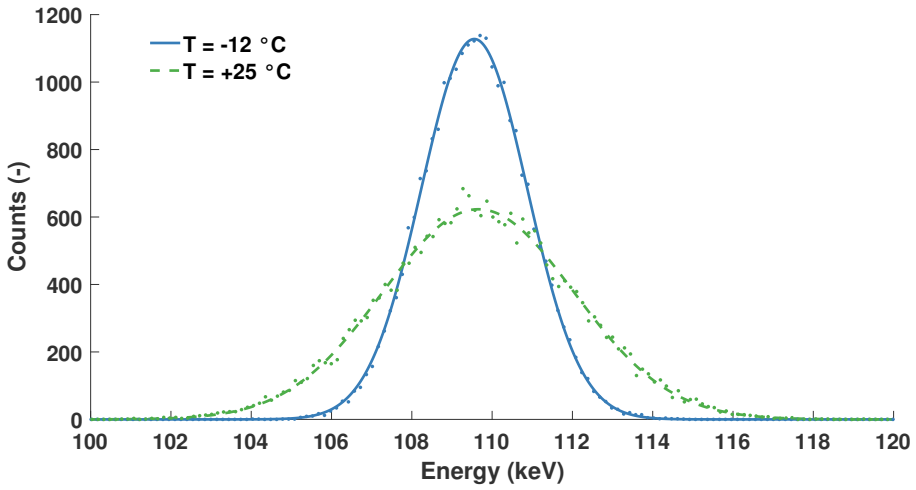

Figure 3. Resulting sensed signal from the detector at the room temperature 25°C and below the freezing point -12°C

Table 1. Resulting detector's FWHM at different temperatures.

Temperature	FWHM
25 °C	4.88 keV
-12 °C	2.87 keV

4. Conclusion

Timepix, the CMOS detector allows imaging and measuring of radiation spectra at the same time. The proposed modification of the detector connection and sense of the generated signal potentially enables to expand the detection spectrum to lower energies. The verification measurements were performed in this arrangement, where the detector works as the single pixel detector. Then we got additive improvement of sensed signal FWHM by another modification of this detector. The thermal stabilisation and even only slight cooling effect of the detector brings a reduction of FWHM. The resulting FWHM was decreased by 2 keV when the temperature was reduced by 37°C. That means the resulting spectral resolution is 2,9 keV for the detector with capacitance 100 pF for the whole (single) pixel.

Acknowledgements. This work was performed in cooperation with the companies Rigaku Innovative Technologies Europe, s.r.o. and ADVACAM s.r.o.. It was supported by the Grant Agency of the Czech Technical University in Prague, grant No. SGS16/169/OHK3/2T/13 and by GA CR grant 13-33324S.

References

Baca, T., Platkevic, M., Jakubek, J., et al. 2016, *Journal of Instrumentation*, **11**, C10007

Blazek, M., Pata, P., Inneman, A., & Skala, P. 2017, *Advances in Astronomy*, **2017**, 316289

Dániel, V., Inneman, A., Pína, L., et al. 2017, in Proceedings of the SPIE, Vol. 10235, EUV and X-ray Optics: Synergy between Laboratory and Space

Dániel, V., Pína, L., Inneman, A., et al. 2016, in Proceedings of the SPIE, Vol. 9978, CubeSats and NanoSats for Remote Sensing, 99780D

Daniel, V., Urban, M., Nentvich, O., & Stehlikova, V. 2016, in Proceedings of the SPIE, Vol. 9978, CubeSats and NanoSats for Remote Sensing, 99780N

Esposito, M., Jakubek, J., Mettivier, G., et al. 2011, *Nuclear Instruments and Methods in Physics Research A*, **652**, 458

Frojdh, E., Campbell, M., De Gaspari, M., et al. 2015, *Journal of Instrumentation*, **10**, C01039

Holik, M., Kraus, V., Georgiev, V., & Granja, C. 2016, *Journal of Instrumentation*, **11**, C02032

Hudec, R., Pina, L., Inneman, A., & Tichy, V. 2015, in Proceedings of the SPIE, Vol. 9510, EUV and X-ray Optics: Synergy between Laboratory and Space IV, 95100A

Jansen, F., Lumb, D., Altieri, B., et al. 2001, *Astronomy and Astrophysics*, **365**, L1

Llopart, X., Ballabriga, R., Campbell, M., Tlustos, L., & Wong, W. 2007, *Nuclear Instruments and Methods in Physics Research A*, **581**, 485

Merloni, A., Predehl, P., Becker, W., et al. 2012, *ArXiv e-prints*

Pina, L., Hudec, R., Inneman, A., et al. 2015, in Proceedings of the SPIE, Vol. 9510, EUV and X-ray Optics: Synergy between Laboratory and Space IV, 951005

Pína, L., Hudec, R., Inneman, A. J., et al. 2016, in Proceedings of the SPIE, Vol. 9964, Advances in Laboratory-based X-Ray Sources, Optics, and Applications V, 99640B

Platkevic, M. 2014, PhD thesis, Czech Technical University in Prague

Platkevic, M., Jakubek, J., Vykydal, Z., & Granja, C. 2011, *Journal of Instrumentation*, **6**, C11023

Poikela, T., Plosila, J., Westerlund, T., et al. 2014, *Journal of Instrumentation*, **9**, C05013

Schwartz, D. A. 2014, *Review of Scientific Instruments*, **85**, 061101

Turecek, D., Jakubek, J., & Soukup, P. 2016, *Journal of Instrumentation*, **11**, C12065

Urban, M., Nentvich, O., Stehlikova, V., et al. 2016, *submitted to Acta Astronautica*

Urban, M., Nentvich, O., Stehlíková, V., & Sieger, L. 2017, in EUV and X-ray Optics: Synergy between Laboratory and Space, Proceedings of the SPIE

Weisskopf, M. C., Tananbaum, H. D., Van Speybroeck, L. P., & O'Dell, S. L. 2000, in Proceedings of the SPIE, Vol. 4012, X-Ray Optics, Instruments, and Missions III, ed. J. E. Truemper & B. Aschenbach, 2–16

Wolter, H. 1952, *Annalen der Physik*, **445**, 94